

# Burst of strongly polarized maser emission at 1612 MHz in the proto-planetary nebula OH17.7–2.0

M. Szymczak<sup>1</sup> and E. Gérard<sup>2</sup>

<sup>1</sup> Toruń Centre for Astronomy, Nicolaus Copernicus University, Gagarina 11, 87-100 Toruń, Poland  
e-mail: msz@astro.uni.torun.pl

<sup>2</sup> GEPI, UMR 8111, Observatoire de Paris, 5 place J. Janssen, 92195 Meudon Cedex, France

Received 20 January 2005 / Accepted 16 February 2005

**Abstract.** We report the discovery of a burst of highly polarized OH maser emission at 1612 MHz in the proto-planetary nebula candidate OH17.7–2.0. The total flux density of two red-shifted features at 72.8 and 73.3 km s<sup>-1</sup> increased nearly threefold over a period of ~430 days. This burst was not associated with any systematic changes of the other 1612 MHz maser features as well as of the 1665 and 1667 MHz masers. The burst was characterized by a linear growth of left-hand circularly polarized emission accompanied by considerable linearly polarized emission. During the burst, the degrees of circular and linear polarization increased up to -80% and 15% respectively. A relation found between the line width and the peak flux density of the two bursting features implies a saturated amplification. Among several possible causes of the burst, a local propagation effect due to Zeeman overlap initiated by evolutionary changes in the shell appears most plausible.

**Key words.** polarization – masers – stars: AGB and post-AGB – circumstellar matter – stars: individual: OH17.7–2.0 – radio lines: stars

## 1. Introduction

Several observational studies of OH17.7–2.0, since its discovery as a strong OH 1612 MHz maser source (Bowers 1978), have provided abundant evidence that it has the characteristics of a proto-planetary nebula (PPN), with a small amplitude (0.16 mag) OH light curve of approximate period 890 days (Herman & Habing 1985). Disappearance of H<sub>2</sub>O maser emission (Engels 2002) and non-detection of SiO maser emission (Nyman et al. 1998) indicate its post-AGB nature. This is consistent with its bimodal infrared energy distribution similar to that observed in young planetary nebulae (Le Bertre 1987). The near-infrared dust imaging has revealed a prolate spheroid with a dense equatorial plane (Bains et al. 2003). They found that OH masers are contained in this equatorial plane. The central star of OH17.7–2.0 has spectral type earlier than K5 with effective temperature ( $T_{\text{eff}}$ ) in the range 4000–10<sup>4</sup> K (Le Bertre et al. 1989).

Herman & Habing (1985) monitored OH17.7–2.0 at 1612 MHz over a period of 4 years from 1978 and detected only small flux-density variations. The shape and intensity of the 1612 MHz profile appear to be very stable over the last three decades (Bowers 1978; Likkell 1989; Bains et al. 2003). IRAS measurements indicated that OH17.7–2.0 is non-variable; the percentage likelihood of variability, estimated from the 12 and 25  $\mu\text{m}$  flux densities obtained generally at 2 week and 6 month intervals, is 21. Likewise, non-variability or only slight

amplitude variations at near-infrared wavelengths were reported by Le Bertre et al. (1989).

During the survey of PPN candidates with the Nançay telescope (Szymczak & Gérard 2004, hereafter SG04) we accidentally noted a rise of the 1612 MHz flux density of red-shifted features near 73 km s<sup>-1</sup> in OH17.7–2.0. The present paper provides the results of nearly 3 years polarimetric observations which cover a quiet phase and an outstanding burst of red-shifted features. Possible causes of this burst of strongly polarized OH masers are discussed.

## 2. Observations and results

OH17.7–2.0 has been monitored since 2002 February (JD = 2452 326) at 1612 and 1667 MHz and since 2003 October (JD = 2452 924) at 1665 MHz using the Nançay radio telescope. Both transitions were simultaneously observed in full polarization mode with spectral resolutions of 0.07 or 0.14 km s<sup>-1</sup>. At each epoch the target was observed for 20 to 40 min in frequency switching mode, so that a noise level ( $1\sigma$ ) of the final Stokes  $I$  spectra was always better than 150 mJy for 0.07 km s<sup>-1</sup> resolution. The characteristics of the instrument and observing procedures to get all four Stokes parameters  $I, Q, U$  and  $V$  were described in detail in SG04. Great care was taken to measure the instrumental polarization. The continuum source 3C 161 and line source W12 were regularly

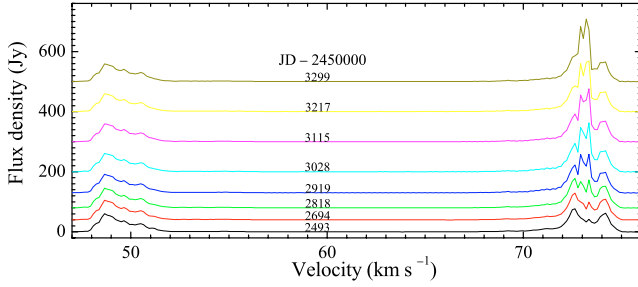


**Fig. 1.** Selected 1612 MHz spectra of the total flux density (Stokes  $I$ ) of OH17.7–2.0 illustrating the variability of features near  $73 \text{ km s}^{-1}$ . Each spectrum is annotated with the truncated julian date (JD–2 450 000) of observation.

observed in order to provide a continuous calibration data set. The calibration is estimated to be uncertain by  $\sim 3\%$ .

The OH data reported in this paper cover a period of  $\sim 1000$  days. Sample 1612 MHz spectra of the Stokes  $I$  parameter taken with a spectral resolution of  $0.14 \text{ km s}^{-1}$  are shown in Fig. 1. This clearly shows a growth of maser features near  $73 \text{ km s}^{-1}$ , whereas the shape and intensity of the blue-shifted part of the spectrum and the rest of red-shifted features are very stable over the observing interval. Data taken with  $0.07 \text{ km s}^{-1}$  resolution allowed us to conclude that the red-shifted part of the 1612 MHz spectrum can be fitted by at least 6 Gaussian components.

Full polarization 1612 MHz spectra at the first epoch of observation (JD = 2 452 326) were published in SG04. We did not find any change in the polarization profiles within errors with the remarkable exception of two red-shifted features at  $72.8$  and  $73.3 \text{ km s}^{-1}$ . The temporal variations of these features in the total flux density (Stokes  $I$ ), circularly polarized flux density (Stokes  $V$ ), linearly polarized flux density ( $p = \sqrt{Q^2 + U^2}$ ) and polarization position angle ( $\chi$ ), are shown in Fig. 2. For comparison purposes, we also plot the variations of the strongest blue-shifted feature at  $48.7 \text{ km s}^{-1}$  and two red-shifted features at  $72.6$  and  $74.1 \text{ km s}^{-1}$  (just bracketting the bursting features). The errors bars are not shown for the sake of clarity. Typical errors are  $2.5\%$  for the peak flux density and  $4^\circ$  for the polarization position angle. Note that Fig. 2 contains data taken with a spectral resolution of  $0.14 \text{ km s}^{-1}$ .

Until JD = 2 452 493, all 1612 MHz features varied nearly together with an amplitude of  $0.16 \text{ mag}$  ( $15\%$ ). This behaviour was observed throughout the whole observing interval for all but the  $72.8$  and  $73.3 \text{ km s}^{-1}$  features. From JD = 2 452 669 to JD = 2 453 102, the flux densities of these features increased linearly with time. Their peak flux densities ( $S_p$ ) in the Stokes  $I$  are best fitted by the expression

$$S_p = 0.28(t - 2446), \quad (1)$$

where  $t$  is the truncated julian date (JD–2 450 000). Over 430 days, these features increased by factors of 2.6 and 2.9, respectively.

Figure 2 (Stokes  $V$ ) clearly illustrates that this growth was almost entirely due to left-hand circularly (LHC) polarized emission. The circular polarization of the two bursting features

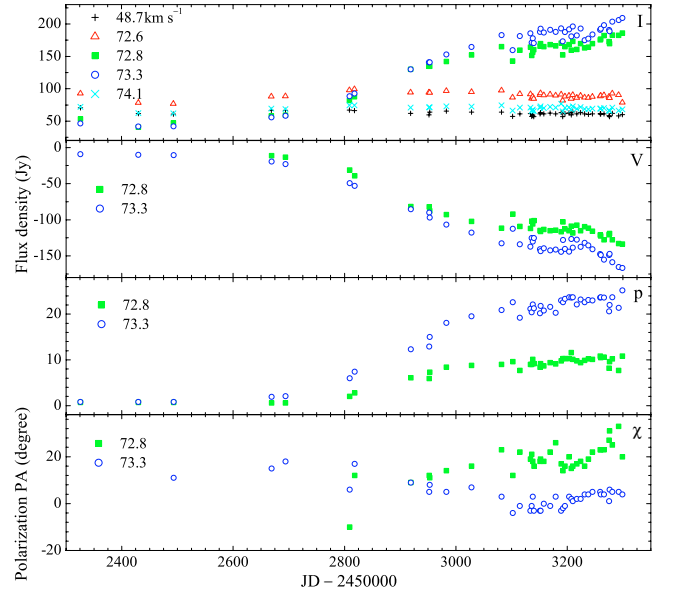


**Fig. 2.** Variations of the peak flux density at 1612 MHz for spectral features (designated by their velocities) in Stokes  $I$ ,  $V$ ,  $p = \sqrt{Q^2 + U^2}$  parameters and of the polarization position angle ( $\chi$ ).

at  $72.8$  and  $73.3 \text{ km s}^{-1}$  varied in the same manner. At the beginning of the burst (JD = 2 452 669), their degrees of circular polarization ( $m_c = V/I$ ) were  $-22\%$  and  $-35\%$  respectively and increased up to  $-70\%$  at the end of the linear growth. Later,  $m_c$  further increased to  $-80\%$ .

A rise of the linearly polarized emission (parameter  $p$ ) of the  $73.3 \text{ km s}^{-1}$  feature followed that seen in Stokes  $V$ ; the rise of the  $72.8 \text{ km s}^{-1}$  feature was not as steep (Fig. 2). The  $p$  flux densities of the  $72.8$  and  $73.3 \text{ km s}^{-1}$  features increased 15 and 30 times, respectively, while the degrees of linear polarization ( $m_l = p/I$ ) increased from  $2\text{--}3\%$  up to  $13\text{--}15\%$ .

The position angles of linearly polarized emission ( $\chi$ ) of the bursting features showed small ( $16\text{--}20^\circ$ ) but systematic changes during the observing interval (Fig. 2).

As the burst phenomenon was essentially due to the rise of LHC maser emission, we have analyzed the Stokes  $V$  profiles in order to determine a relation of the line width,  $\Delta V$ , (full width at half maximum) versus the peak flux density,  $S_p$ , during the growth phase of the two bursting features. For this purpose we only used data with  $0.07 \text{ km s}^{-1}$  spectral resolution and find

$$\Delta V = 0.01(\pm 0.01)S_p^{0.65(\pm 0.28)}, \quad (2)$$

for the  $72.8 \text{ km s}^{-1}$  feature and

$$\Delta V = 0.03(\pm 0.01)S_p^{0.44(\pm 0.04)}, \quad (3)$$

for the  $73.3 \text{ km s}^{-1}$  feature. We note that the fitting for the first feature (Eq. (2)) was much poorer than for the second feature (Eq. (3)) likely due to a blending effect. These relations imply that there was a saturated growth of circularly polarized emission (Goldreich & Kwan 1974).

Figure 3 shows that the integrated flux density of the blue-shifted emission at 1612 MHz varied with an amplitude of  $0.16 \text{ mag}$ , i.e. exactly the same as reported previously

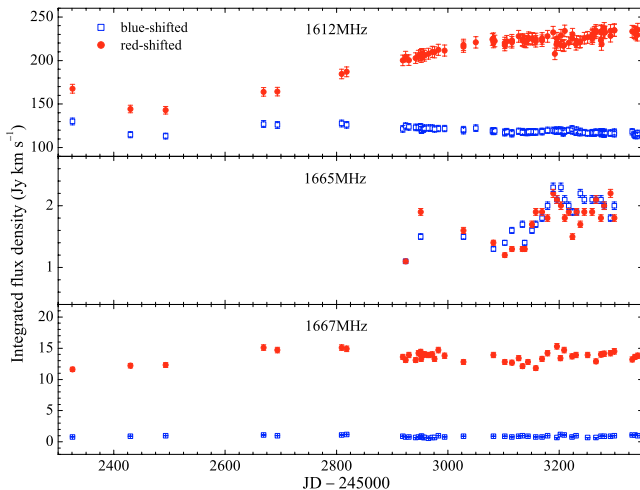


**Fig. 3.** Variations of the integrated flux density at three OH transitions for blue- (squares) and red-shifted (circles) parts of the spectrum.

(Herman & Habing 1985), but without any obvious periodicity. The observations at 1665 MHz started nearly in the middle of the linear growth of the two 1612 MHz features and flux density variations of amplitude 0.7–0.8 mag on time scales of 30–100 days were observed. It is worthwhile to notice nearly the same behaviour of the blue- and red-shifted emissions (Fig. 3). Changes in the 1665 MHz flux density were not correlated with the burst at 1612 MHz. The 1667 MHz emission varied with an amplitude of 0.3–0.7 mag on time scales from tens to hundreds of days. We conclude that the burst of 72.8 and 73.3 km s<sup>-1</sup> at 1612 MHz was not correlated with changes of the other 1612 MHz features as well as with the integrated flux densities of the 1665 and 1667 MHz maser lines.

### 3. Discussion

The fact that only two of the six red-shifted OH 1612 MHz features have undergone through the burst, without any change in the blue-shifted part of the spectrum and in the 1665 and 1667 MHz spectra, is puzzling. The burst in OH17.7–2.0 is spectacular and unique when compared to outburst events in circumstellar OH masers reported in the literature. Almost all OH maser bursts occurred in the envelopes of Mira type variables and are characterized by global changes (at time scales of months and years) in OH profiles at 1612, 1665 and 1667 MHz transitions, if present (e.g. Jewell et al. 1981; Etoke & Le Squeren 1997). Usually, OH flux eruptive changes are not linked to erratic changes in the optical and/or infrared. There is no satisfactory explanation for such phenomena so far. Lewis et al. (1986) reported a strong intensity increase of a single feature at 1612 MHz in the supergiant star IRC+10420 accompanied by a decrease in the flux density of the 1665 MHz feature at the same velocity. This behaviour is interpreted as evidence for a competitive gain effect (Field 1985).

There is general consensus that the 1612 MHz OH maser line is pumped by far-infrared photons (Elitzur et al. 1976). This was confirmed by observations which showed that the maser and IR flux densities vary in phase (e.g. Werner et al. 1980). ISO observations of the IRC+10420 supergiant

directly confirmed that the 34.6  $\mu\text{m}$  photons are involved in the 1612 MHz line pumping (Sylvester et al. 1997). In OH/IR and Miras the 1612 MHz maser is probably pumped by the alternative route, beginning with the 53.3  $\mu\text{m}$  photons (He & Chen 2004). Therefore, if the radiative pumping is dominant in OH17.7–2.0, our observations imply that only a local rise of the infrared flux may correspond to the burst of the two 1612 MHz features. A plausible cause of such a rise can be a rapid increase of the dust formation rate (Soker & Clayton 1999). They proposed a model in which the dynamo magnetic activity results in the formation of cool spots in the AGB stars, such that dust forms more easily. The enhanced local magnetic field can produce episodes of higher mass loss that can develop asymmetric structures. This mechanism can be more effective when a star descends the AGB becoming a proto-planetary nebula. However, it is unclear how fluctuations in mass loss emerged at a distance of a few AU can propagate up to hundreds of AU where OH 1612 MHz masers operate. In the case of OH17.7–2.0, the 1612 and 1667 MHz masers originate from the same remnant AGB shell with inner and outer radii of 1350 and 4590 AU respectively (Bains et al. 2003). If the enhancement of the IR flux is responsible for the 1612 MHz burst, we should observe a concomitant event in the 1667 MHz line as the IR photons are possibly involved in pumping of the both transitions (Collison & Nedoluha 1993). But we should also observe enhancements of all 1612 features and in particular those of the red wing close to the bursting ones namely at 72.6 and 74.1 km s<sup>-1</sup>. This is clearly not the case for our target. We therefore presume that an increase in the IR flux is not likely the cause of the 1612 MHz maser burst. High angular resolution observations of the OH transitions in order to localize the burst in the shell should help to verify this suggestion.

OH17.7–2.0 showed remarkable evolution of its H<sub>2</sub>O maser emission (Engels 2002). The water maser decreased in intensity by a factor of a hundred during the period from 1985 to 1990 and is now undetectable. The disappearance of this maser is interpreted as a consequence of the rapid decrease of the mass loss rate well below a level of 10<sup>-7</sup> M<sub>⊙</sub> yr<sup>-1</sup> (Engels 2002). Assuming that the H<sub>2</sub>O maser originates in the shell of radius of 20–50 AU, and that the decline of the H<sub>2</sub>O maser in 1990 and that the onset of the OH maser flare in 2003 are casually related, we argue that a disturbance that quenched the H<sub>2</sub>O maser reaches the innermost region of the 1612 MHz masers when propagating with a speed of ~500 km s<sup>-1</sup>. The presence of jet-like outflows (few × 100 km s<sup>-1</sup>) in many young PNe and PPNe was directly confirmed by H $\alpha$  imaging (e.g. Sahai & Trauger 1998). High speed bubbles propagating in the remnant AGB shell can abruptly decrease the number of maser molecules and the coherent maser path length and ultimately destroy the masing conditions. It is very unlikely that the collimated jets may facilitate the maser burst in the standard model of the circumstellar OH maser emission (Elitzur et al. 1976). However, there are several arguments (see Sect. 1) that our source is initiating its evolutionary way to the PN stage where at some point it is going to develop axisymmetric or/and multipolar outflows. In such a case, it is not impossible that these outflows could give rise to new OH masers in other locations (closer to the star) than predicted in the standard model and

with a totally different velocity field. High angular resolution studies are clearly needed to test this possibility. But again, it is a priori surprising that the adjacent velocity features at 72.6 and 74.1 km s<sup>-1</sup> remained unaffected during the outburst.

A modulation of mass loss rate across the envelope as well as inhomogeneity in the circumstellar matter due to the above discussed mechanisms can significantly affect the shielding of H<sub>2</sub>O and OH molecules against UV photons. The photodissociation of H<sub>2</sub>O molecules is regarded as an effective mechanism of OH molecule production (e.g. Huggins & Glassgold 1982). Estimates of  $T_{\text{eff}}$  of OH17.7–2.0 are uncertain but even for an upper value of <10<sup>4</sup> K, the photodissociation by the stellar UV photons gives a small contribution to the production of OH. However, if  $T_{\text{eff}}$  is high enough to dissociate H<sub>2</sub>O molecules but too low to photodissociate OH molecules, one could expect the disappearance of H<sub>2</sub>O masers and rise of OH masers. This possibility, however, cannot explain the burst of the 1612 MHz OH features without associated changes at other radial velocities and other OH transitions.

Assuming that the bursting features lay in the standard OH maser location, i.e. at the H<sub>2</sub>O photodissociation radius, these red-shifted velocities cannot be amplifying the stellar continuum. We hypothesize that the observed increase of the OH maser flux density by about 150 Jy could be a result of amplification of the emission from an extra galactic background source. If this is the case, the flux of the background source would be 150/e<sup>τ</sup> Jy. For τ = 10 we obtain 7 mJy. In order to test this possibility, we must detect a source at the position of the bursting maser components and find a correlation between their flux densities. This case can be considered as very appealing since it would give us a direct measurement of the optical depth of the maser.

Our observations show that the burst at 72.6 and 74.1 km s<sup>-1</sup> is not accompanied by changes at other velocities and that similar bursts are not seen at 1665 and 1667 MHz. This suggests that the burst is confined to a limited part of the envelope and can be a propagation effect. The hypothesis of a propagation effect is supported by our data as the OH emission of the bursting features is strongly circularly polarized ( $m_c$  up to 80%). Theories predict that OH circular polarization is created by a Zeeman effect involving magnetic fields of the order of few mG when the splitting of magnetic components of the ground rotational state is higher than the Doppler line width. Under certain conditions (for instance the matching of the gradients of the velocity and of the magnetic field in the maser region, e.g. Cook (1966) or the overlap of Zeeman components alone) the observed strong polarization is a result of the amplification of one sense of circularly polarized emission. Amplification of only one  $\sigma$  component of the Zeeman pair was postulated in OH maser models (Deguchi & Watson 1986; Elitzur 1996) and can produce high circular polarization up to 100% due to the magnetic beaming (Gray & Field 1994). The presence of linearly polarized emission but of moderate degree of polarization  $m_l$  up to 13–15% suggests that the OH emission is in fact elliptically polarized. Using the model of Deguchi & Watson, we found that the polarization characteristics of the 1612 MHz burst are consistent with the representative saturated case (their Fig. 1) for an angle

of ~60° between the magnetic field and the axis of the velocity gradients and for a ratio of Zeeman splitting to Doppler line width  $x_B = 2$ . Polarimetric high angular resolution observations of the 1612 MHz in OH17.7–2.0 (Bains et al. 2003) revealed a magnetic field of strength of +4.6 mG. Such a field strength is sufficient to account for the above ratio of  $x_B$ . It is worthwhile noting that the velocity separation between the 1612 MHz bursting features is 0.5 km s<sup>-1</sup>, nearly half the velocity separation of the Stokes +V and -V extrema identified as a Zeeman pair by Bains et al. (2003) in their I<sub>12</sub>02 feature at nearly the same radial velocity. One might suggest that the 72.8 and 73.3 km s<sup>-1</sup> bursting features are Zeeman components which should increase together during the outburst. But again, VLBI studies are clearly needed to verify this hypothesis. We conclude that the burst of strongly polarized OH emission can be well explained by the Zeeman overlap. However, with this interpretation, it is difficult to explain why such phenomena are not observed more often.

A good knowledge of the position and polarization parameters of the bursting OH region from follow up high angular resolution studies will no doubt allow us to verify some of the possible interpretations discussed above. One possibility may be that the Zeeman overlap is enhanced as separate maser bubbles come to coincide along the line-of-sight to the observer, due to internal motions.

*Acknowledgements.* The Nancay Radio Observatory is the Unité Scientifique de Nancay of the Observatoire de Paris, associated with the CNRS. The Nancay Observatory gratefully acknowledges the financial support of the Region Centre in France.

## References

- Bains, I., Gledhill, T. M., Yates, J. A., & Richards, A. M. S. 2003, MNRAS, 338, 287
- Bowers, P. F. 1978, A&AS, 31, 127
- Cook, A. H. 1966, Nature, 211, 503
- Collison, A. J., & Nedoluha, G. E. 1993, ApJ, 413, 735
- Deguchi, S., & Watson, W.D. 1986, ApJ, 300, L15
- Elitzur, M. 1996, ApJ, 457, 415
- Elitzur, M., Goldreich, P., & Scoville, N. 1976, ApJ, 205, 384
- Engels, D. 2002, A&A, 388, 252
- Etoka, S., & Le Squeren, A. M. 1997, A&A, 321, 877
- Field, D. 1985, MNRAS, 217, 1
- Goldreich, P., & Kwan, J. 1974, ApJ, 190, 27
- Gray, M. D., & Field, D. 1994, A&A, 292, 693
- He, J. H., & Chen, P. S. 2004, New Astron., 9, 545
- Herman, J., & Habing, H. J. 1985, A&AS, 59, 523
- Huggins, P. J., & Glassgold, A. E. 1982, AJ, 87, 1828
- Jewell, P. R., Webber, J. C., & Snyder, L. E. 1981, ApJ, 249, 118
- Le Bertre, T. 1987, A&A, 180, 160
- Le Bertre, T., Epchtein, N., Gouiffes, C., Heydari-Mayaleri, M., & Perrier, C. 1989, A&A, 225, 417
- Lewis, B. M., Terzian, Y., & Eder, J. 1986, ApJ, 302, L23
- Likkel, L. 1989, ApJ, 344, 350
- Nyman, L. A., Hall, P. J., & Olofsson, H. 1998, A&AS, 127, 185
- Sahai, R., & Trauger, J. T. 1998, AJ, 116, 1357
- Soker, N., & Clayton, G. C. 1999, MNRAS, 307, 993
- Sylvester, R. J., Barlow, M. J., Nguyen-Q-Rieu, et al. 1997, MNRAS, 291, L42
- Szymczak, M., & Gérard, E. 2004, A&A, 423, 209 (SG04)
- Werner, M. W., Beckwith, S., Gatley, I., et al. 1980, ApJ, 239, 540